ARTICLE
Journal of Cellular Biochemistry 115:1752–1761 (2014)

Journal of Cellular Biochemistry

MicroRNA-365 Inhibits the Proliferation of Vascular Smooth Muscle Cells by Targeting Cyclin D1

Myung-Hyun Kim,[1] Onju Ham,[2,3] Se-Yeon Lee,[2,3] Eunmi Choi,[4] Chang Youn Lee,[5] Jun-Hee Park,[5] Jiyun Lee,[2,3] Hyang-Hee Seo,[2,3] Minji Seung,[2,3] Eunhyun Choi,[6] Pil-Ki Min,[1] and Ki-Chul Hwang[2,3,4]*

[1]*Cardiology Division, Heart Center, Gangnam Severance Hospital, Yonsei University College of Medicine, Republic of Korea*

[2]*Cardiovascular Research Institute, Yonsei University College of Medicine, Republic of Korea*

[3]*Brain Korea 21 PLUS Project for Medical Science, Yonsei University College of Medicine, Republic of Korea*

[4]*Severance Biomedical Science Institute, Yonsei University College of Medicine, Republic of Korea*

[5]*Department of Integrated Omics for Biomedical Sciences, Graduate School, Yonsei University, Republic of Korea*

[6]*Severance Integrative Research Institute for Cerebral & Cardiovascular Disease, Yonsei University Health System, Republic of Korea*

ABSTRACT

Abnormal proliferation of vascular smooth muscle cells (VSMCs) is a common feature of disease progression in atherosclerosis. Cell proliferation is regulated by cell cycle regulatory proteins. MicroRNAs (miR) have been reported to act as important gene regulators and play essential roles in the proliferation and migration of VSMCs in a cardiovascular disease. However, the roles and mechanisms of miRs in VSMCs and neointimal formation are far from being fully understood. In this study, cell cycle-specific cyclin D1 was found to be a potential target of miR-365 by direct binding. Through an in vitro experiment, we showed that exogenous miR-365 overexpression reduced VSMC proliferation and proliferating cell nuclear antigen (PCNA) expression, while miR-365 was observed to block G1/S transition in platelet-derived growth factor-bb (PDGF-bb)-induced VSMCs. In addition, the proliferation of VSMCs by various stimuli, including PDGF-bb, angiotensin II (Ang II), and serum, led to the downregulation of miR-365 expression levels. The expression of miR-365 was confirmed in balloon-injured carotid arteries. Taken together, our results suggest an anti-proliferative role for miR-365 in VSMC proliferation, at least partly via modulating the expression of cyclin D1. Therefore, miR-365 may influence neointimal formation in atherosclerosis patients. J. Cell. Biochem. 115: 1752–1761, 2014.

KEY WORDS: MIR-365; VASCULAR SMOOTH MUSCLE CELLS; PROLIFERATION; CELL CYCLE; CYCLIN D1

Vascular smooth muscle cells (VSMCs) compose the major structure of the vasculature, and play roles such as maintaining vessel tone and blood pressure [Sarkar et al., 2006]. Under normal conditions, VSMCs are retained in a non-proliferative state (G0) before vascular injury. However, after vessel injuries such as atherosclerosis and restenosis, VSMCs re-enter the cell cycle for proliferation and accumulation in response to stimulatory growth factors and cytokines such as PDGF-bb, interleukin-1, interleukin-6, and tumor necrosis factor-alpha [Liu et al., 2011; Marx et al., 2011]. Injured VSMCs re-enter the cell cycle with increased rates of proliferation and migration, while SMC proliferation and migration play crucial roles in the pathogenesis of atherosclerosis [Ferguson

Abbreviations used: miR, microRNA; miR-365, microRNA-365; VSMCs, vascular smooth muscle cells; Ang II, angiotensin II; PCNA, proliferating cell nuclear antigen; PDGF-bb, platelet-derived growth factor-bb.

The authors declared that they have no conflicts of interest.

Grant sponsor: Korean government (MEST); Grant numbers: 2011-0019243, 2011-0019254; Grant sponsor: Korea Health 21 R&D Project, Ministry of Health & Welfare, Republic of Korea; Grant number: A0120478.

*Correspondence to: Ki-Chul Hwang, Severance Biomedical Science Institute, Cardiovascular Research Institute, Yonsei University College of Medicine, 250 Seongsanno, Seodamun-gu, Seoul 120-752, Republic of Korea.
E-mail: kchwang@yuhs.ac

Manuscript Received: 14 November 2013; Manuscript Accepted: 8 May 2014

Accepted manuscript online in Wiley Online Library (wileyonlinelibrary.com): 12 May 2014

DOI 10.1002/jcb.24841 • © 2014 Wiley Periodicals, Inc.

3rd and Patterson, 2003]. Studies of molecular mechanisms to modulate cell cycle-dependent SMC proliferation are of paramount importance.

MicroRNAs (miRs) are endogenous, small (20–25 nucleotides) non-coding RNAs that control gene expression post-transcriptionally by targeting mRNAs and binding to complementary sequences in their 3′ untranslated regions (UTR) [Ambros, 2004; Bartel, 2009]. Increasing evidences indicate that miRs modulate important cellular processes including survival, proliferation, apoptosis, and development [Hwang et al., 2006]. Recent studies suggest that miRs also play essential roles in the control of VSMC function and phenotype in cardiovascular disease [Parmacek, 2009; Kang et al., 2012]. In particular, miR-21, -145, -143, -133, -221, and -222 are indicated to play pivotal roles in SMC functions and proliferation. Inhibition of miR-21 decreases the proliferation of VSMCs as well as injured rat carotid artery by targeting PTEN [Ji et al., 2007], and knockdowns of miR-221 and miR-222 decrease VSMC proliferation and migration in vitro by targeting cyclin-dependent kinase (CDK) inhibitors, p27 and p57, respectively [Liu et al., 2009]. MiR-143 and 145 are highly expressed in VSMCs and are downregulated in response to PDGF-bb [Cordes et al., 2009]. Furthermore, the overexpression of miR-145 inhibits not only VSMC proliferation but also neointimal formation in balloon injury models by targeting the transcription factor KLF5 [Rangrez et al., 2011]. MiR-133 has also been indicated to reduce VSMC proliferation and migration by suppressing the expression of transcription factor Sp-1 [Chen et al., 2011].

A previous study demonstrated that miR-365 inhibits the proliferation of lung cancer and colon cancer cells, and modulates ox-LDL-induced apoptosis in endothelial cells [Torella et al., 2011; Wang et al., 20012; Merlet et al., 2013]. However, the role of miR-365 in the proliferation of VSMCs is not fully understood. In the present study, we first found that miR-365 decreased proliferation induced by PDGF-bb via a direct interaction between miR-365 and the 3′UTR of rat cyclin D1 mRNA. Indeed, miR-365 is significantly downregulated in proliferating rat VSMCs and after balloon-injury to the carotid artery. Taken together, our data suggest that miR-365 may be a useful therapeutic tool to inhibit VSMC proliferation and migration in vascular disease.

MATERIALS AND METHODS

ISOLATION AND CULTURE OF RAT AORTIC VSMCs

Rat aortic VSMCs were isolated as previously described [Kim et al., 2012]. All experimental procedures for animal studies were performed according to protocols approved by the Committee for the Care and Use of Laboratory Animals, Yonsei University College of Medicine, and performed in accordance with the Committee's Guidelines and Regulations for Animal Care (NIH Publication No. 85-23, revised 1996). Thoracic aortas from 6- to 8-week-old Sprague-Dawley rats were removed and transferred to serum-free Dulbecco's modified Eagle's medium (DMEM; Invitrogen Co, Carlsbad, CA) containing 100 U/ml of penicillin and 100 μg/ml of streptomycin. The aorta was freed from the connective tissue, and then transferred into a Petri dish containing 5 ml of an enzyme dissociation mixture containing DMEM with 1 mg/ml of collagenase type I (Sigma, St. Louis, MO) and 0.5 μg/ml elastase (USB Bioscience, Cleveland, OH), and incubated for 30 min at 37 °C. The aorta was transferred to DMEM, and the adventitia was stripped off with forceps under a microscope. The aorta was transferred into a conical tube containing 5 ml of the enzyme dissociation mixture and incubated for 2 h at 37 °C. The suspension was centrifuged at 1500 rpm for 10 min, and the pellet was resuspended in DMEM with 10% fetal bovine serum (FBS). Rat aortic VSMCs were cultured in DMEM supplemented with 10% FBS in 75 cm^2 flasks in a 37 °C incubator at 5% CO_2 (Forma Scientific, Inc., Marjetta, OH).

CELL PROLIFERATION ASSAY

VSMCs were plated in triplicate wells of 96-well plates at 1×10^4 cells per well. The cells were starved with 0.1% FBS for 24 h and then treated with PDGF-bb, angiotensin II, or serum. After treatment, cell proliferation was measured using a CCK-8 assay kit (Dojindo, Japan). The CCK-8 assay kit was diluted with DMEM, and then 100 μl was added to each well and incubated for 2 h at 37 °C. The absorbance was measured at 450 nm with a spectrometer.

CELL CYCLE ANALYSIS

The distribution of VSMCs at different stages in the cell cycle was estimated by flow cytometry. Briefly, cells were seeded in DMEM containing 10% FBS and then starved in serum-free medium for one day. Cells were transfected with or without miRNA mimic and stimulated with PDGF-bb (20 ng/ml) for 24 h. After treatment, cells were harvested and washed with phosphate-buffered saline (PBS; pH 7.4) and fixed with 70% ethanol diluted in PBS at 4 °C. Following PBS washing, the pellet was dissolved in RNase A solution (20 μg/ml) and incubated at 37 °C for 15 min. Cells were stained with propidium iodide (PI) for 30 min and analyzed using Fluorescence-activated cell sorting (FACS) analysis (Becton Dickinson, San Jose, CA). The percentage of cells in each cell cycle phase was analyzed using the ModFit LT program.

MICRORNA TRANSFECTION

Mature rat miRs and negative control RNA oligomers (N.C, Genolution Pharmaceuticals, Inc., Seoul, Korea) were used at a final concentration of 50 nM. The sequence of the mature miR mimic was as follows: miR-365: 5′-UAAUGC CCCUAAAAAUCCUUAU-3′. VSMCs were transfected with miR mimics using siLentFect(TM) Lipid reagent (BioRad, Hercules, CA) in high glucose DMEM containing 10% FBS and after 4 h incubation in a CO_2 incubator at 37 °C, the medium was changed.

REVERSE TRANSCRIPTION POLYMERASE CHAIN REACTION (RT-PCR)

Single-stranded cDNA was synthesized from total RNA using a reverse transcription system (Promega, Madison, WI) according to the manufacturer's instructions. Briefly, a 20 μl RT reaction mixture containing 1 μg total RNA, 1x RT buffer (10 mM Tris/HCl, pH 9.0, 50 mM KCl and 0.1% Triton X-100), 1 mM deoxynucleoside triphosphates (dNTPs), 20 unit RNase inhibitor, 0.5 μg oligo (dT) 15, and 10 units reverse transcriptase was incubated at 42 °C for 15 min, heated to 99 °C for 5 min, and incubated at 4 °C for 5 min. PCR was performed for 30 cycles with 3′ and 5′ primers based on the sequences of cyclin D1. RT-PCR products were separated by

electrophoresis on a 1.2% agarose gel (BioRad). Glyceraldehyde-3-phosphate dehydrogenase (GAPDH) was used as an internal standard, and the signal intensity of the amplified product was normalized to that of GAPDH.

REAL-TIME PCR

Total RNAs were isolated with the use of Trizol reagent (Invitrogen, Grand Island, NY). miRNAs were assayed by real-time PCR. The cDNAs were produced from 100 ng purified total RNA with Taqman® MicroRNA Reverse Transcriptase Kit (Applied Biosystems, Foster City, CA) in combination with Taqman® MicroRNA Assays for quantification of specific miR-365, according to the manufacturer's conditions. U6 was used as an endogenous control for data normalization. Real-time PCR analyses for amplification and detection of specific miRNAs were performed in a Light Cycler 480 II (Roche) at 95 °C for 10 min, followed by 40 cycles of 95 °C for 15 s, and 60 °C for 60 s. The relative differences in expression levels of miRNA in VSMCs ($\Delta\Delta$Ct) were calculated and presented as fold induction ($2^{-\Delta\Delta Ct}$) after normalization to control U6.

IMMUNOBLOT ANALYSIS

Cells were washed once in PBS and extracted using a lysis buffer (Cell Signaling Technology, Boston, MA) containing 20 mM Tris/HCl (pH 7.5), 150 mM NaCl, 1 mM Na_2EDTA, 1 mM EGTA, 1% Triton X-100, 2.5 mM sodium pyrophosphate, 1 mM β-glycerophosphate, 1 mM Na_3VO_4, 1 mg/ml leupeptin and 1 mM PMSF. Protein concentrations were determined using a BCA protein assay kit (Pierce Biotechnology, Rockford, IL). Proteins were separated in a 10% SDS-polyacrylamide gel and transferred to PVDF membranes (Millipore, Billerica, MA). After blocking the membrane with TBS-T (TBS-Tween 20; 0.1% Tween 20) containing 5% (w/v) non-fat dried skimmed milk powder for 1 h at room temperature, membranes were washed twice with TBS-T and incubated with primary antibody for 1 h at room temperature or overnight at 4 °C. The membrane was washed three times with TBS-T for 10 min and incubated with horseradish peroxidase (HRP)-conjugated secondary antibody for 1 h at room temperature. After extensive washing, bands were detected using ECL western blotting detection reagent (Amersham Biosciences, Japan). The band intensities were quantified using Image J. The cyclin D1 (HD11) and PCNA (PC10) antibodies were purchased from Santa Cruz Biotechnology (Dallas, TX).

LUCIFERASE ACTIVITY ASSAY

The predicted targeting miRNAs of cyclin D1 were retrieved using a publicly available database (TargetScan, www.targetscan.org). We synthesized the 3′ UTR of cyclin D1, which contained the predicted binding sites for miR-365. The corresponding genes were then cloned into the XhoI/XbaI site of pmirGLO vector (Promega). VSMCs were plated at 1×10^5 cells/well in 12-well plates. After 24 h, the pmirGLO vector containing the cyclin D1 binding site for miRNAs was co-transfected with miR-365 or control miRNA. Renilla luciferase was used to normalize the cell number and the transfection efficiency. Luciferase activity was measured using the dual luciferase assay (Promega, Fitchburg, WI) according to the manufacturer's instructions after 24 h on the luminometer.

WOUND-HEALING ASSAY

VSMCs were plated at a density of 3×10^5 cells/well in 6-well plates. After the cells had reached 80% confluence, cells were deprived of serum for 24 h and then incubated with mitomycin C (10 μg/ml, dissolved in culture medium), a potent inhibitor of cell proliferation, for 2 h. After incubation, the cells were wounded with 200 μl pipette tips and the starting points were marked with a marker pen at the bottom of the plates. The medium was replaced with or without serum-deprived medium-containing PDGF-bb (20 ng/ml), and the cells were incubated for 16 h. Images were captured using an Axiovert 40 °C inverted microscope (Carl Zeiss, Thornwood, NY) equipped with a Powershot A640 digital camera (Canon, Osaka, Japan).

MIGRATION ASSAY

VSMCs (8×10^3 cells) were seeded into the upper chamber of a Transwell filter with 8 μm pores (Costar Corning) coated with 10 μg/ml fibronectin. The cells were deprived of serum for 16 h, and stimulating medium-containing PDGF-bb (20 ng/ml) was added to the lower chamber. Transwell chambers were incubated at 37 °C for 16 h. After incubation, cells on the underside of the filter were stained with coomassie brilliant blue. Non-migrating cells on the upper side of the filter were removed with cotton swabs.

RAT CAROTID ARTERY BALLOON INJURY MODEL

Balloon injury was performed as previously described [Tulis, 2007]. Briefly, under zoletil (20 mg/kg) and rompum (5 mg/kg) anesthesia, the left carotid artery was isolated and a 2-Fr Fogarty balloon catheter (Baxter Healthcare Corp., Irvine, CA) was introduced through an external carotid arteriotomy incision, advanced to the aortic arch, inflated to produce moderate resistance, and gradually withdrawn three times. Then, the catheter was removed and the proximal external carotid artery was ligated. Sham operations were performed on the right common carotid arteries. At 7 days after balloon injury, rats were anesthetized and the carotid arteries were excised. This study was performed according to a protocol approved by the Institutional Animal Care and Use Committee of Yonsei University in accordance with the Guide for the Care and Use of Laboratory Animals.

LOCAL OLIGONUCLEOTIDE DELIVERY INTO VASCULAR WALL

To deliver miR-365 mimic and N.C to the vascular tissue after balloon injury, we applied an established local oligonucleotide delivery model via F-127 pluronic gel (Sigma, St. Louis, MO) as described by Xiaojun Liu et al [Liu et al., 2011]. Immediately after balloon injury of the right common carotid artery, transfection solution (50 μl 0.2% transfection reagent in Opti-MEM) was mixed with miR-365 mimic and N.C (10 μg) and infused into the ligated segment of the common carotid artery for 30 min. Then, 90 μg of these miRs, preloaded into 200 μl 30% F-127 pluronic gel and 1% transfection reagent at 4 °C, was applied locally to the adventitia around the injured artery segments.

HISTOLOGICAL ANALYSIS

To measure the neointimal areas, aortas were excised from sacrificed rats and perfused with phosphate buffered saline (PBS) to remove blood and then fixed in 10% formalin solution for 24 h at 4 °C.

Sequentially, tissue sections were mounted onto gelatin-coated glass slides to guarantee that different stains could be used on successive tissue sections cut through the injury area. After the sections were deparaffinized and rehydrated, they were stained with hematoxylin and eosin (H&E) to estimate neointimal areas and quantified using NIH Image J software version 1.34e. Collagen was also analyzed using Masson's Trichrome staining. Proliferating cells were stained by PCNA and cyclin D1. In brief, samples were blocked in 2.5% normal horse serum and incubated with anti-PCNA or anti-cyclin D1 antibody. Biotinylated pan-specific universal secondary antibody and streptavidin/peroxidase complex reagent were used to treat the sections. Using the DAB substrate kit, the sections were stained with antibody. Counterstaining was performed with 1% methyl green and dehydration was conducted with 100% n-butanol, ethanol, and xylene before mounting in VectaMount Mounting Medium. FITC-conjugated goat anti-rabbit IgG (Jackson ImmunoResearch Laboratories, West Grove, PA) was used as the secondary antibody for cyclin D1. A coverslip was placed on top of each section and the sections were observed using light microscopy. The images for trichrome stain, H&E, and PCNA were obtained by virtual microscopy (BX51/dot Slide, Olympus, Tokyo, Japan) Images for cyclin D1 was detected using laser scanning confocal microscopy and transferred to a computer equipped with MetaMorph software (version 4.6). The areas are expressed as percentages of the total left ventricle. Fibrosis was also analyzed by Masson's trichrome staining. For quantification, five slices of each group were prepared and five different regions per slice were chosen for observation.

STATISTICAL ANALYSIS

Results are expressed as mean ± SD from at least three independent experiments. Statistical analyses were performed using Student's *t*-test. Comparisons between more than two groups were performed by one-way ANOVA using Bonferroni's correction. Relationships were considered statistically significant when the *P*-value was less than 0.05.

RESULTS

MiR-365 INHIBITS VSMCs PROLIFERATION TREATED WITH PDGF-BB

To substantiate the hypothesis that miRs have potential inhibitory effects on VSMC proliferation for modulating the cell cycle, we aimed to regulate G1/S-specific cyclin D1 expression using miRs in

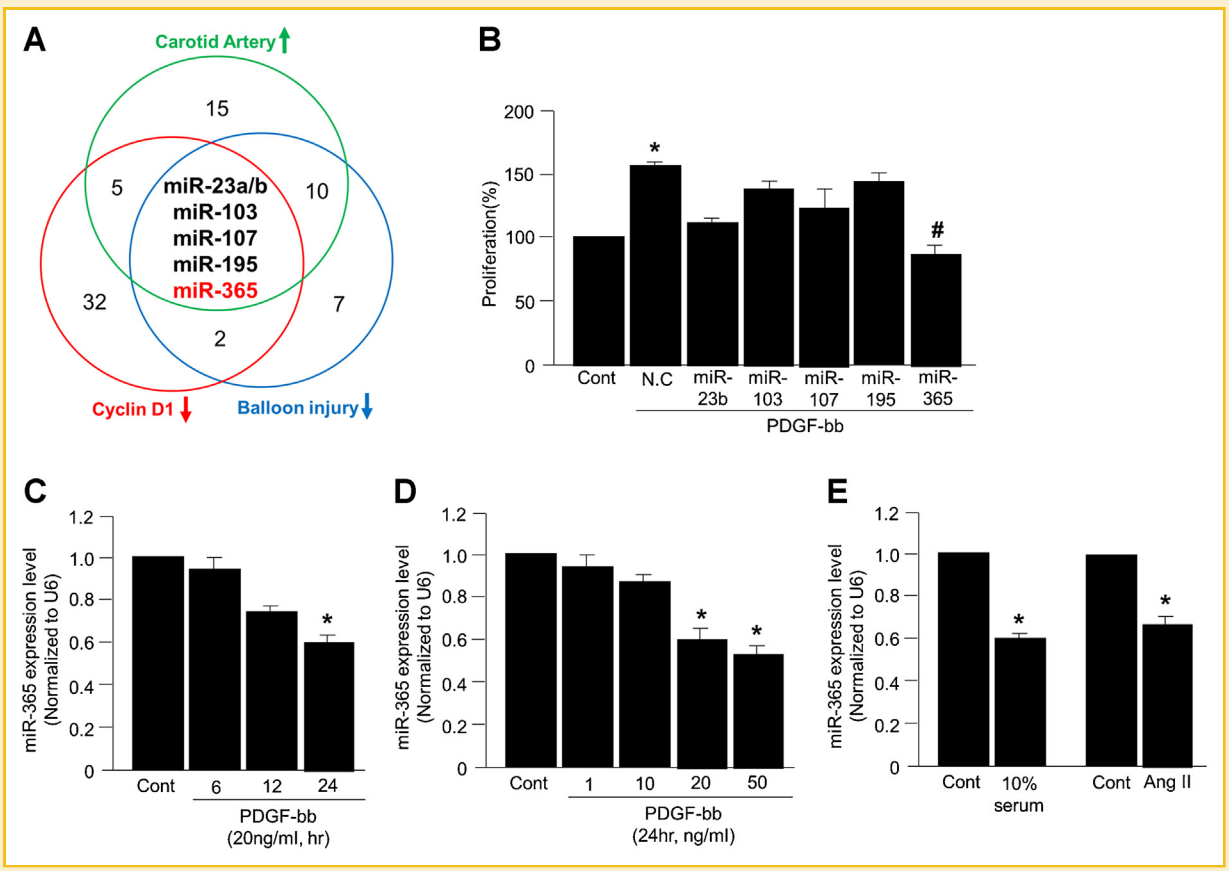

Fig. 1. The effect of miR-365 in VSMC proliferation. Venn diagram illustrating the predicted miRNAs targeting cyclin D1 (red circle), miRNAs highly expressed in normal rat carotid artery (green circle), and miRNAs significantly downregulated after injury (blue circle) (A). VSMC proliferation was measured by the CCK-8 assay (B). VSMCs were treated with PDGF-bb (20ng/ml) for 24 h. PDGF-bb caused time- and dose-dependent decreases in endogenous miR-365 expression in VSMCs, as determined by real-time PCR (C,D). Real-time PCR results showed the change of miR-365 expression in 10% serum or Ang II (100 nM)-stimulated VSMCs (E). (*$P < 0.05$ vs. control, #<0.05 vs. PDGF-bb-treated VSMCs).

rat carotid balloon injury models in vivo and PDGF-bb-treated VSMCs in vitro. Cyclin D1 plays important roles in the regulation of cell proliferation and in the neointimal formation of balloon-injured vascular walls [Diehl et al., 2002; Findeisen et al., 2011]. To identify miRNAs that may regulate cyclin D1-mediated VSMC proliferation, we searched for putative miRs that are able to target cyclin D1 based on a prediction program, TargetScan. We identified a total of 58 miRs that potentially target cyclin D1. Among these miRs, we focused on those that were: verified in the intersection area; predicted to target cyclin D1; highly expressed in the normal rat carotid artery; and downregulated after injury [Ji et al., 2007]. These miRs were miR-23a/b, miR-103, miR-107, miR-195, and miR-365 (Fig. 1A). To select the most anti-proliferative miR, the five candidate miRs were transfected and treated with PDGF-bb. The data showed that miR-365 highly suppressed VSMC proliferation induced by PDGF-bb (Fig. 1B). Among the five candidate miRs, endogenous miR-23b and miR-195 expression levels were highly decreased in response to PDGF-bb treatment (Supple. Fig. 1A). All miRs had increased expression levels compared to the control upon transfection into cells (Supple. Fig. 1B). However, miR-365 most convincingly suppressed the expression of cyclin D1 in VSMCs treated with PDGF-bb (Supple. Fig. 1C). To examine the change of endogenous miR-365 expression in proliferating VSMCs, PDGF-bb was treated dose- or time-dependently. MiR-365 expression was decreased in a time- and dose-dependent manner after PDGF-bb treatment (Fig. 1C, D). To further verify the expression of miR-365 in several stimuli-treated VSMCs including 10% serum and angiotensin II (Ang II). The data suggested that the expression of miR-365 is decreased in proliferating VSMCs by various stimuli (Fig. 1E).

CYCLIN D1 IS A DIRECT TARGET OF MIR-365 IN VSMCs

To determine the inhibitory effect of miR-365, a miR-365 mimic was transfected into VSMCs, which caused miR-365 expression levels to be significantly increased (Fig. 2A). To determine whether miR-365

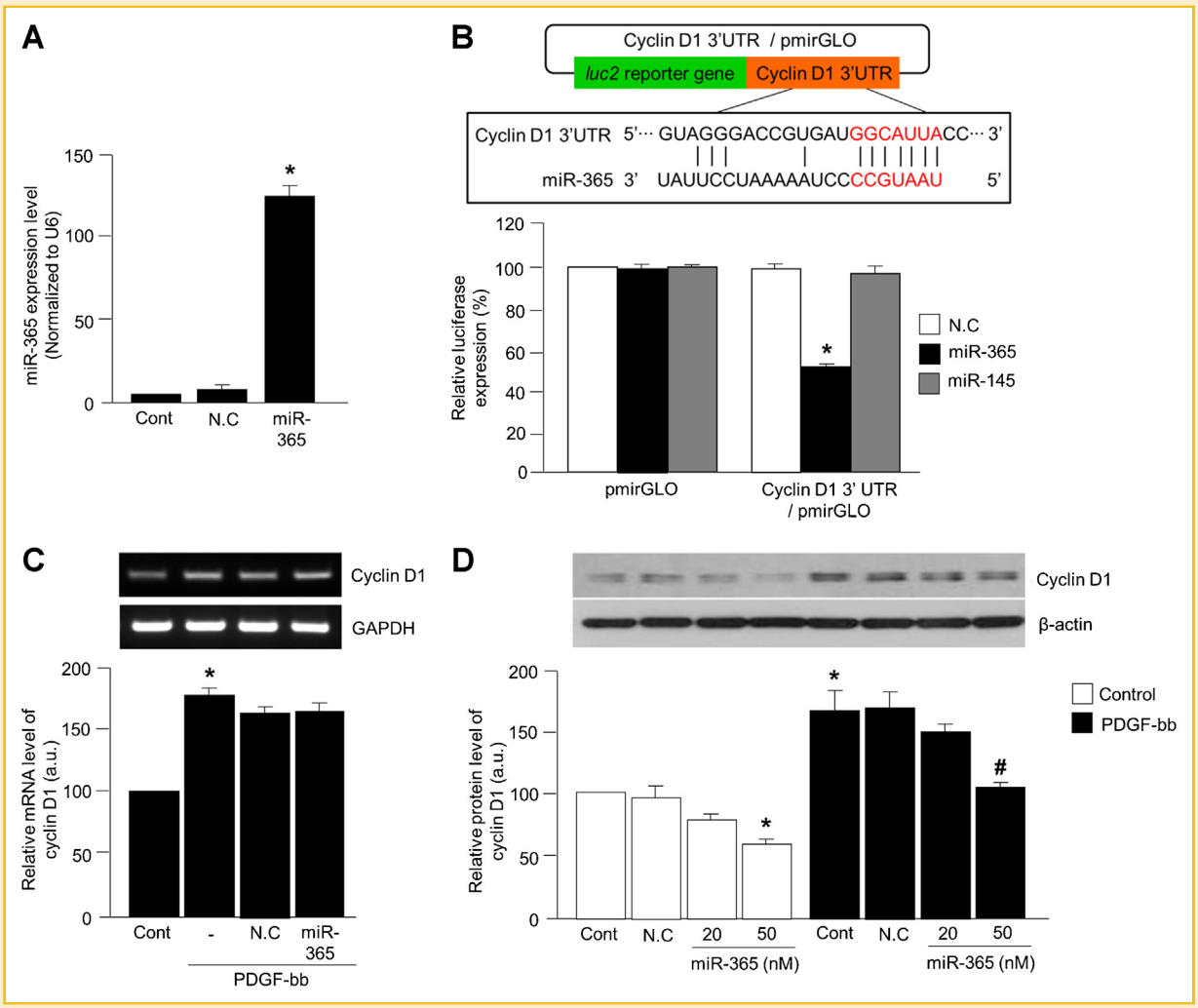

Fig. 2. Identification of cyclin D1 as a direct target of miR-365 in VSMCs. Transfection efficiency was detected by real-time PCR. Negative Control (N.C) miRNA or miR-365 (100 nM) was transfected in VSMCs (A). A rat cyclin D1 3′ UTR containing the miR-365 binding sequence was cloned into a luciferase reporter gene. Luciferase activity was assessed by the dual luciferase assay and the renilla activity was measured for normalized N.C. (B). The mRNA level of cyclin D1 was analyzed by RT-PCR. GAPDH was used as a control (C). VSMCs transfected with N.C. or miR-365 mimic were stimulated with PDGF-bb (20 ng/ml) and analyzed for the cyclin D1 protein by western blot. β-actin was used as a control (D). (*$P < 0.05$ vs.control, #<0.05 vs. PDGF-bb-treated VSMCs).

directly binds to the 3′ UTR sequence of rat cyclin D1 mRNA and affects its expression, the 3′ UTR sequence of cyclin D1 containing the putative binding site for miR-365 was cloned into a luciferase reporter vector. The construct vector was then co-transfected with miR-365 mimics into VSMCs. The luciferase assay was inhibited in cells transfected with miR-365 compared to that with N.C. and miR-145 (a miRNA with a well-known inhibitory effect on VSMCs proliferation, but that does not bind to the 3′ UTR of cylin D1) (Fig. 2B). To further verify that cyclin D1 is a functional target gene of miR-365 in rat VSMCs, we transfected VSMCs with either N.C. (as a control) or a miR-365 mimic, and the expression levels of cyclin D1 mRNA were determined by RT-PCR. Interestingly, PDGF-bb increased mRNA levels of cyclin D1, but miR-365 had no effect (Fig. 2C). As determined by western blot analysis, overexpression of miR-365 downregulated both basal and PDGF-bb-induced cyclin D1 expression in VSMCs (Fig. 2D). The results show that miR-365 regulated the protein expression of cyclin D1 but did not alter the mRNA levels, indicating that cyclin D1 is post-transcriptionally regulated by miR-365.

MiR-365 CONTROLS CELL CYCLE IN PROLIFERATING VSMCs

Next, we investigated the role of miR-365 in proliferating VSMCs treated with several stimuli. VSMC proliferation was induced by PDGF-bb, 10% serum, or Ang II (Fig. 3A–C). Proliferation was constrained in miR-365-transfected cells. The proliferating cell nuclear antigen (PCNA) that plays a crucial role in the life and death decisions of cells, was also investigated. Representative expression of PCNA was significantly decreased in miR-365-overexpressed VSMCs compared to cells treated with PDGF-bb (Fig. 3D). Indeed, miR-365-overexpressed cells exhibited significantly increased S phase population compared to cells that were treated with N.C. MiR-365 played a critical role for entering the G1/S phase transition in PDGF-bb-induced cell-cycle progression (Fig. 3E). To confirm the effect of the blockage of miR-365, we used artificial anti-miR-365 mimics. We found no distinctive changes in the proliferation, and expression of cyclin D1 and PCNA, in anti-miR-365-transfected SMCs (Supple. Fig. 2). Moreover, anti-miR-365 had no effect on the migration of PDGF-bb-treated SMCs (Supple. Fig. 3).

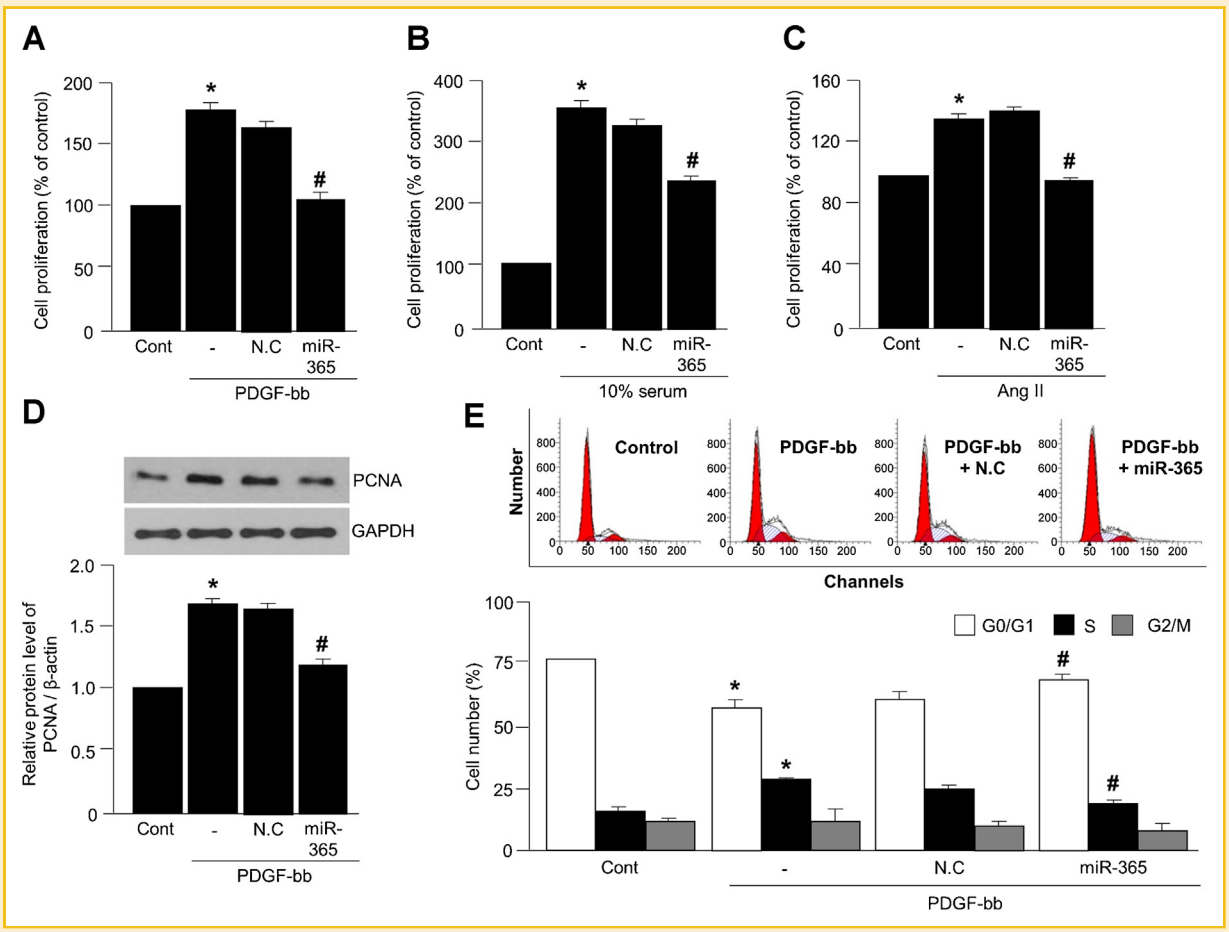

Fig. 3. The anti-proliferative effects of miR-365 in VSMCs. VSMCs were transfected with N.C or miR-365, and then treated with or without PDGF-bb (20 ng/ml) (A), 10% serum (B), or Ang II (100 nM) (C). CCK-8 assays were used to assess the effects of exogenous miR-365 mimic in VSMCs treated with various stimuli. PCNA expression was measured using western blotting and protein level of PCNA was normalized by β-actin. VSMCs were transfected with N.C as a control miRNA or miR-365 mimic, and then treated with PDGF-bb (20 ng/ml) (D). Cell cycle profiles were determined by FACS analysis (stained with PI). The histograms in panel A were analyzed by the ModFit LT program to determine the percentages of cells in the G0/G1, S, and G2/M phases of the cell cycle (E). (*$P < 0.05$ vs. control, #<0.05 vs. PDGF-bb-treated VSMCs).

MiR-365 SUPPRESSES VSMCs MIGRATION AND PROLIFERATION

PDGF-bb is a well-known growth factor of cell proliferation, and is a key factor in migration from the media to intima in injured vessels [Ross, 1993; Cai et al., 2012]. To confirm the inhibitory effect of miR-365, a Boyden chamber assay was performed (Fig. 4A). The number of migratory cells was suppressed in miR-365-overexpressed VSMCs compared to cells treated with PDGF-bb. To confirm the inhibitory effect of miR-365 on proliferating VSMCs, a wound healing assay was performed. The wound-healing assay revealed that PDGF-bb-treated VSMCs covered more than twofolds of the wound compared to the control, whereas miR-365-transfected VSMCs were able to suppress proliferation (Fig. 4B).

MiR-365 REGULATES NEOINTIMAL FORMATION AFTER BALLOON INJURY

The expression levels of miR-365 in rat balloon injury (B.I) models, characteristic of neointimal formation indicative of VSMC proliferation, was measured by real-time PCR. At 7 days after balloon injury, endogenous miR-365 expression was significantly decreased (Fig. 5A). To determine the anti-proliferative role of miR-365 in VSMCs, miR-365 was transfected using a gel transfection system after balloon injury. Endogenous expression of cyclin D1 showed a 10-fold increase compared to the control; however, the miR-365-transfected groups showed decreased expression of cyclin D1 (Fig. 5B). Overexpression of miR-365 highly inhibited neointimal formation compared to the group transfected with N.C after balloon injury (Fig. 5C,D). Overexpression of miR-365 showed a decrease of PCNA expression in neointimal formation compared to the N.C-transfected group (Fig. 5E). In order to confirm the change of cyclin D1 expression after B.I, we performed immunofluorescence staining. Figure 5F shows that cyclin D1 was highly expressed in the balloon injury model, while miR-365 suppressed the expression of cyclin D1. Taken together, the results reveal that miR-365 targets cyclin D1 in the G1 phase of the cell cycle in VSMCs treated with PDGF-bb. Endogenous miR-365 was downregulated in proliferating VSMCs by various stimuli such as PDGF-bb, serum, and Ang II. MiR-365 regulates G1/S transition in PDGF-bb-induced VSMCs and modulates expression of PCNA in vivo and in vitro. Overexpression of miR-365 suppresses proliferation and migration of VSMCs in vitro and in vivo by targeting cyclin D1 (Fig. 5G).

DISCUSSION

Abnormal proliferation of VSMCs is associated with atherosclerosis and restenosis following balloon angioplasty [Liu et al., 2011; Marx et al., 2011]. Accumulating research suggests that miRs are an emerging class of small RNAs that regulates gene expression, and shows important roles in VSMC proliferation and migration [Parmacek, 2009; Bartel, 2011]. miRs, noncoding RNA molecules, comprise a small number nucleotides and regulate biological processes including the modulation of stem cell self-renewal, differentiation, apoptosis, and proliferation via regulating post-transcription or translation by binding to the 3′UTR of target genes [Ambros, 2004; Bartel DP., 2009; Cai et al., 2012]. However, the mechanism by which miRs achieve these functions needs further

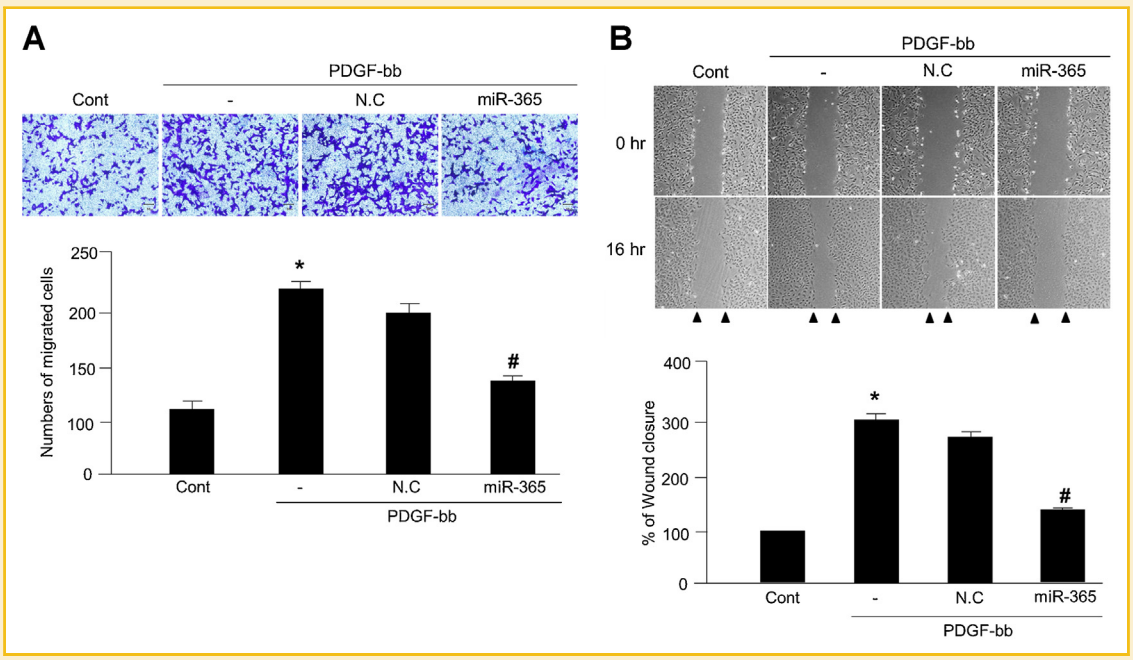

Fig. 4. The effect of miR-365 on VSMC migration. Photographs of VSMCs from the underside of a Boyden chamber (A). Number of migrated VSMCs were counted using a microscope and the representative fields (x 100) are shown (B). Analysis of cell migration measured by a wound-healing assay (Top). Representative images were taken at 0 h and 16 h post-wound (x 200) (Bottom). The wound closure was quantified at 16 h and normalized by measuring the remaining unmigrated area using Image J (*$P < 0.05$ vs. control, #<0.05 vs. PDGF-bb-treated VSMCs).

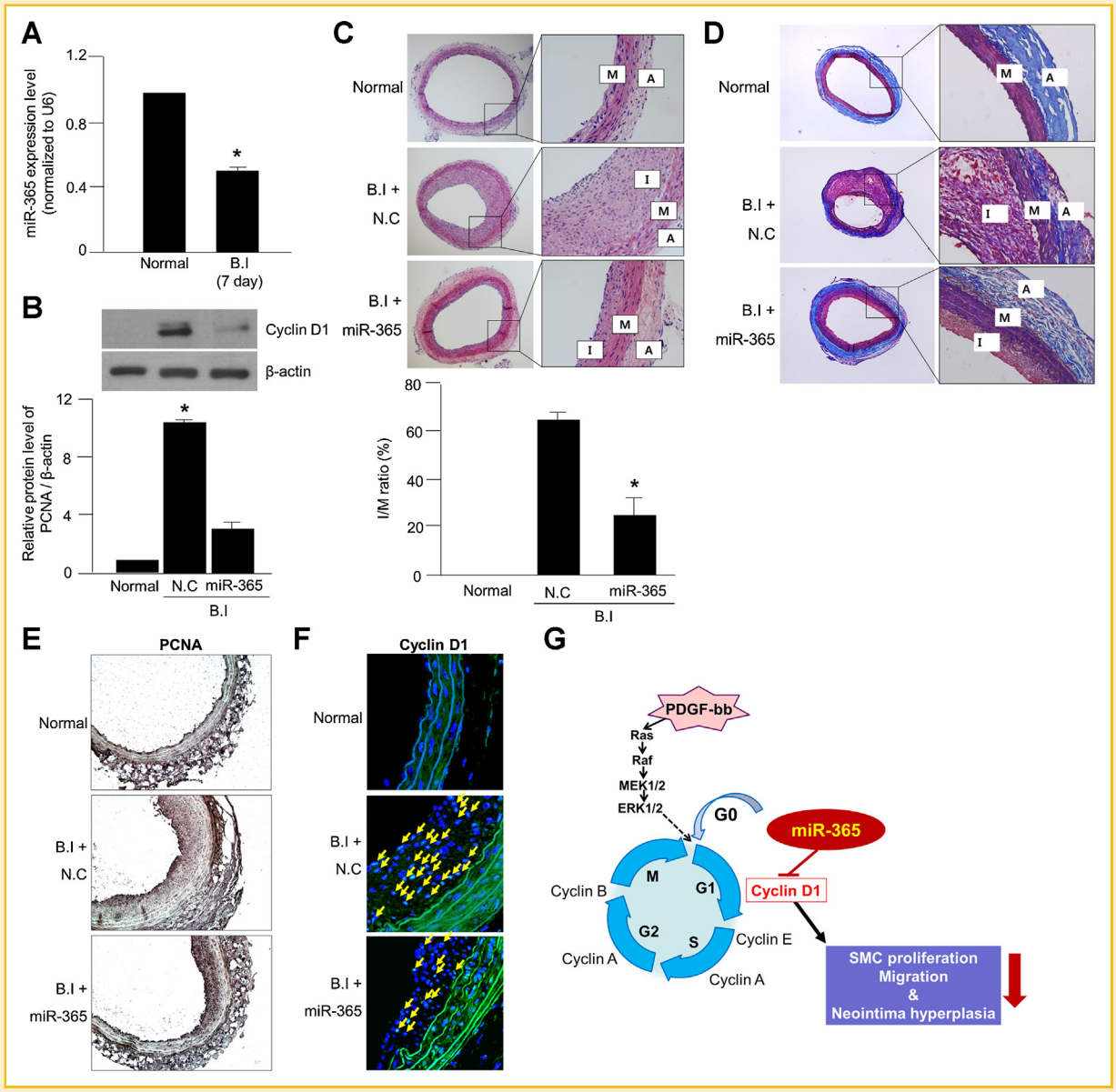

Fig. 5. The change of miR-365 expression in rat balloon injury model. The expression of endogenous miR-365 was detected by real-time PCR and normalized to U6, which was used as an internal control (A). The expression of cyclin D1 in normal, and negative control or miR-365-transfected balloon injury models was analyzed by western blot. β-actin was used as a control (B). Hematoxylin and eosin staining (H&E staining) and trichrome staining were performed to confirm the inhibition of neointimal formation by miR-365 (C, D). Immunohistochemistry was performed in order to detect the change of PCNA expression (E). Confocal images of IF staining for DAPI (blue) and cyclin D1 (green) in normal, and negative control or miR-365-transfected balloon injury model (F). A schematic diagram shows the role of miR-365 in VSMCs stimulated with PDGF-bb via targeting cyclin D1 (G). (*$P < 0.05$ vs. normal). $N = 5$ for each group.

study. Recent studies of VSMC proliferation indicate that miR-195 inhibits oxidized low-density lipoprotein (oxLDL)-induced VSMC proliferation by repressing the expression of cell division cycle 42 (Cdc42), cyclin D1, and fibroblast growth factor 1 (FGF1) [Wang et al., 2012]. MiR-424/322 overexpression showed to inhibit serum-stimulated VSMC proliferation, and resulted in decreased expression of cyclin D1 and Ca^{2+}-regulating protein calumenin [Merlet et al., 2013]. Also, VSMC phenotype and neointimal formation were found to be regulated by miR-663 [Li et al., 2013]. With this, a recent publication revealed that miR-365 exhibited a more significant decrease in expression than miR-195 after injuries, and was previously reported to inhibit proliferation of VSMCs [Ji et al., 2007]. Various roles of miR-365 have been reported. miR-365 potentiates ox-LDL-induced endothelial cell apoptosis by regulating the expression of Bcl-2, and inhibits cell-to-cell adhesion and proliferation in tumor cell types, including lung cancer and colon cancer, by targeting polycystic kidney and hepatic disease gene 1 (PKHD1), cyclin D1, Bcl-2, or NK2 homeobox 1 (NKX21) [Qin et al.,

2011; Duan et al., 2012; Nie et al., 2012; Kang et al., 2013]. MiR-365 also enhances chondrocyte differentiation by directly targeting histone deacethylase 4 (HDAC4) [Guan et al., 2011]. However, the role of miR-365 in the proliferation of VSMCs remains unknown.

Cyclin D1 is a nuclear protein required for cell cycle regulation in the G1 phase of proliferating cells, and its expression is significantly increased in rat carotid arteries after balloon injury and in proliferating VSMCs under various stimuli, including PDGF-bb and high glucose, in vitro [Karpurapu et al., 2010; Park et al., 2013]. siRNA inhibited PDGF-bb-induced DNA synthesis of cyclin D1 in human SMCs; in contrast, adenovirus-mediated overexpression of cyclin D1 caused proliferation and neointima formation after injury [Karpurapu et al., 2010]. In the present study, we found that miR-365 functions as a regulator in VSMCs by targeting cyclin D1. In miR-365-overexpressed cells, expression levels of cyclin D1 were significantly inhibited via direct binding to the 3′UTR of cyclin D1 mRNA. Furthermore, the G1/S transition was arrested, and proliferation and the proliferation marker, PCNA, were down-regulated despite being treated with stimuli including PDGF-bb, Ang II, and serum.

In conclusion, in the present study we initially identified miR-365 as an inhibitor of VSMC proliferation that blocks the G1/S transition by regulating cyclin D1. MiR-365 expression was markedly downregulated in proliferating VSMCs in response to PDGF-bb. Our results provide information about the novel mechanisms of miR-365 associated with VSMC proliferation and migration by inhibiting cyclin D1. Therefore, our results suggest that miR-365 is a potential therapeutic strategy for the treatment of restenosis and atherosclerosis.

ACKNOWLEDGMENTS

This research was supported by Korea Science and Engineering Foundation Grants funded by the Korean government (MEST) (2011-0019243, 2011-0019254), and a grant from the Korea Health 21 R&D Project, Ministry of Health & Welfare, Republic of Korea (A0120478).

REFERENCES

Ambros V. 2004. The functions of animal microRNAs. Nature 431:350–355.

Bartel DP. 2009. MicroRNAs: target recognition and regulatory functions. Cell 136:215–233.

Cai Y, Knight WE, Guo S, Li JD, Knight PA, Yan C. 2012. Vinpocetine suppresses pathological vascular remodeling by inhibiting vascular smooth muscle cell proliferation and migration. J Pharmacol Exp Ther 343:479–488.

Chen J, Yin H, Jiang Y, Radhakrishnan SK, Huang ZP, Li J, Shi Z, Kilsdonk EP, Gui Y, Wang DZ, Zheng XL. 2011. Induction of microRNA-1 by myocardin in smooth muscle cells inhibits cell proliferation. Arterioscler Thromb Vasc Biol 31:368–375.

Cordes KR, Sheehy NT, White MP, Berry EC, Morton SU, Muth AN, Lee TH, Miano JM, Ivey KN, Srivastava D. 2009. MiR-145 and miR-143 regulate smooth muscle cell fate and plasticity. Nature 460:705–710.

Diehl JA. 2002. Cycling to cancer with cyclin D1. Cancer Biol Ther 1:226–231.

Duan J, Huang H, Lv X, Wang H, Tang Z, Sun H, Li Q, Ai J, Tan R, Liu Y, Chen M, Duan W, Wei Y, Zhou Q. 2012. PKHD1 post-transcriptionally modulated by miR-365-1 inhibits cell-cell adhesion. Cell Biochem Funct 30:382–389.

Ferguson 3rd JE, Patterson C. 2003. Break the cycle: the role of cell-cycle modulation in the prevention of vasculoproliferative diseases. Cell Cycle 2:211–219.

Findeisen HM, Gizard F, Zhao Y, Qing H, Heywood EB, Jones KL, Cohn D, Bruemmer D. 2011. Epigenetic regulation of vascular smooth muscle cell proliferation and neointima formation by histone deacetylase inhibition. Arterioscler Thromb Vasc Biol 31:851–860.

Guan YJ, Yang X, Wei L, Chen Q. 2011. MiR-365: a mechanosensitive microRNA stimulates chondrocyte differentiation through targeting histone deacetylase 4. FASEB J 25:4457–4466.

Hwang HW, Mendell JT. 2006. MicroRNAs in cell proliferation, cell death, and tumorigenesis. Br J Cancer 94:776–780.

Ji R, Cheng Y, Yue J, Yang J, Liu X, Chen H, Dean DB, Zhang C. 2007. MicroRNA expression signature and antisense-mediated depletion reveal an essential role of MicroRNA in vascular neointimal lesion formation. Circ Res 100:1579–1588.

Kang H, Hata A. 2012. MicroRNA regulation of smooth muscle gene expression and phenotype. Curr Opin Hematol 19:224–231.

Kang SM, Lee HJ, Cho JY. 2013. MicroRNA-365 regulates NKX2-1, a key mediator of lung cancer. Cancer Lett 335:487–494.

Karpurapu M, Wang D, Van Quyen D, Kim TK, Kundumani-Sridharan V, Pulusani S, Rao GN. 2010. Cyclin D1 is a bona fide target gene of NFATc1 and is sufficient in the mediation of injury-induced vascular wall remodeling. J Biol Chem 285:3510–3523.

Kim JS, Kim IK, Lee SY, Song BW, Cha MJ, Song H, Choi E, Lim S, Ham O, Jang Y, Hwang KC. 2102. Anti-proliferative effect of rosiglitazone on angiotensin II-induced vascular smooth muscle cell proliferation is mediated by the mTOR pathway. Cell Biol Int 36:305–310.

Li P, Zhu N, Yi B, Wang N, Chen M, You X, Zhao X, Solomides CC, Qin Y, Sun J. 2013. MicroRNA-663 regulates human vascular smooth muscle cell phenotypic switch and vascular neointimal formation. Circ Res 113:1117–1127.

Liu MW, Roubin GS, King 3rd. SB. 2011. Restenosis after coronary angioplasty. Potential biologic determinants and role of intimal hyperplasia. Circulation 79:1374–1387.

Liu X, Cheng Y, Zhang S, Lin Y, Yang J, Zhang C. 2009. Necessary role of miR-221 and miR-222 in vascular smooth muscle cell proliferation and neointimal hyperplasia. Circ Res 104:476–487.

Liu XJ, Cheng YH, Chen XW, Yang J, Xu L, Zhang CX. 2011. MicroRNA-31 regulated by the extracellular regulated kinase is involved in vascular smooth muscle cell growth via large tumor suppressor homolog 2. J Biol Chem 286:42371–42380.

Marx SO, Totary-Jain H, Marks AR. 2011. Vascular smooth muscle cell proliferation in restenosis. Circ Cardiovasc Interv 4:104–111.

Merlet E, Atassi F, Motiani RK, Mougenot N, Jacquet A, Nadaud S, Capiod T, Trebak M, Lompré AM, Marchand A. 2013. MiR-424/322 regulates vascular smooth muscle cell phenotype and neointimal formation in the rat. Cardiovasc Res 98:458–468.

Nie J, Liu L, Zheng W, Chen L, Wu X, Xu Y, Du X, Han W. 2012. MicroRNA-365, down-regulated in colon cancer, inhibits cell cycle progression and promotes apoptosis of colon cancer cells by probably targeting Cyclin D1 and Bcl-2. Carcinogenesis 33:220–225.

Park ES, Lee KP, Jung SH, Lee DY, Won KJ, Yun YP, Kim B. 2013. Compound K, an intestinal metabolite of ginsenosides, inhibits PDGF-BB-induced VSMC proliferation and migration through G1 arrest and attenuates neointimal hyperplasia after arterial injury. Atherosclerosis 228:53–60.

Parmacek MS. 2009. MicroRNA-modulated targeting of vascular smooth muscle cells. J Clin Invest 119:2526–2528.

Qin B, Xiao B, Liang D, Xia J, Li Y, Yang H. 2011. MicroRNAs expression in ox-LDL treated HUVECs: MiR-365 modulates apoptosis and Bcl-2 expression. Biochem Biophys Res Commun 410:127–133.

Rangrez AY, Massy ZA, Metzinger-Le Meuth V, Metzinger L. 2011. MiR-143 and miR-145: molecular keys to switch the phenotype of vascular smooth muscle cells. Circ Cardiovasc Genet 4:197–205.

Ross R. 1993. The pathogenesis of atherosclerosis: a perspective for the 1990s. Nature 362:801–809.

Sarkar K, Sharma SK, Sachdeva R, Romeo F, Garza L, Mehta JL. 2006. Coronary artery restenosis: vascular biology and emerging therapeutic strategies. Expert Rev Cardiovasc Ther 24:543–556.

Torella D, Iaconetti C, Catalucci D, Ellison GM, Leone A, Waring CD, Bochicchio A, Vicinanza C, Aquila I, Curcio A, dorelli G, Indolfi C. 2011. MicroRNA-133 controls vascular smooth muscle cell phenotypic switch in vitro and vascular remodeling in vivo. Circ Res 109:880–893.

Tulis DA. 2007. Rat carotid artery balloon injury model. Methods Mol Med 139:1–30.

Wang YS, Wang HY, Liao YC, Tsai PC, Chen KC, Cheng HY, Lin RT, Juo SH. 2012. MicroRNA-195 regulates vascular smooth muscle cell phenotype and prevents neointimal formation. Cardiovasc Res 95:517–526.

SUPPORTING INFORMATION

Additional supporting information may be found in the online version of this article at the publisher's web-site.